- ¹ Mokhtar Said
- 2,4* Doaa A. Gad
- ³*Ali M. El-Rifaie
- ⁴Ahmed A.M. El Gaafary
- ^{4,5} Adel A. Elbaset
- ⁶ Mohammed Morad

Performance of RIME Algorithm for Optimal Sizing of Design Hybrid Wind Turbine-Photovoltaic-Battery System



Abstract: - In developing nations, many remote areas use internal combustion generators as their primary source of power, as a result, energy is costly in these places. Therefore, hybrid renewable energy systems (HRESs) like wind turbine (WT) and photovoltaic (PV) offer a cost-effective way to distribute electricity in these locations. However, because of the unreliability in determining the output power of these resources, a battery energy storage system is utilized. This research study optimizes photovoltaic/wind turbine/battery (PV/WT/Batt) HRES that is connected to a standalone micro-grid to supply the energy needs of residential housing and industrial units in the Egyptian city of Siwa, Egypt. The optimum sizing of hybrid system is applied based on RIME algorithm. A fitness function is used to minimize the loss of power supply probability (LPSP). The decision variables of optimization problem (including number of PV arrays and WTs) are optimized for having a high-performance reliable system. From the results, optimal HRES system is made up of 98 PV arrays, 187 wind turbines, and 414 batteries. The designed HRES delivers exceptional performance, with no unmet loads and a relatively low cost of energy (COE) and LSPS.

Keywords: Optimization; RIME; LPSP; Photovoltaic; Wind Turbine.

1. Introduction

The use of fossil fuels as energy sources leads to enormous expansions in hazardous emissions and environmental pollution [1]. Consequently, global pollution in the year 2020 is 5.9% lower than in 2019 due to energy consumption reduction during the COVID-19 pandemic outbreak [2]. As a result, efforts were concentrated on developing dependability of the electricity supply through use of hybrid renewable energy systems (HRES), which utilizes sources of clean energy such as solar power, biomass, wind, fuel cells and hydropower, Furthermore, due to the rapid grow of power need and inability of regular plants to meet the demand, HRESs can be used to close the difference between demand and supply loads or to provide power to remote areas [3-8]. In Egypt, the available hybrid renewable energy resources like solar and wind energy provide alternative sustainable energy source [9].

One of most important aspects of the hybrid systems is optimal sizing that various studies have been carried out on. In the literature, J. Li et al. (2023) [10] applied MATLAB software for simulating and applying a proposed bi-level technique to determine optimal sizing of hybrid wind-photovoltaic-hydrogen and minimize the levelized cost of storage while ensuring the optimal total annual cost. C. A. W. Ngouleu et al. (2023) [11] introduced the Cuckoo search algorithm to optimally size PV-wind turbine generator-diesel generator hybrid system to fulfill load demands of three non-domestic loads in Cameroon at various sites in highly affordable and trustworthy approach. Fayza S. Mahmoud et al. (2022) [12] employed grey wolf optimizer, salp swarm algorithm, and the improved grey wolf

mohammedmoradsalama@gmail.com Copyright © JES 2024 on-line: journal.esrgroups.org

¹ Electrical Engineering Department, Faculty of Engineering, Fayoum University, Fayoum 43518, Egypt. msi01@fayoum.edu.eg (M.S.)

^{2*}Corresponding author: Electrical Engineering Department, Future High Institute of Engineering, Fayoum 63511, Egypt. doaagad.pg@eng.s-mu.edu.eg

³*Corresponding author: College of Engineering and Technology, American University of the Middle East, Egaila 54200, Kuwait; ali,elrifaie@aum.edu.kw

⁴ Electrical Engineering Department, Faculty of Engineering, Minia University, El-Minia, Egypt; elgaafary@mu.edu.eg

⁵Department of Electromechanics Engineering, Faculty of Engineering, Heliopolis University, Cairo, Egypt; Adel.soliman@mu.edu.eg ⁶ Electrical Engineering and Computers Engineering Dep., Higher Institute of Engineering and Technology, New Minya, Egypt;

techniques to dedicate optimal sizing wind/PV turbines/ diesel / battery generators hybrid system to lower energy cost and the loss of power supply probability (LPSP). J. Li et al. (2022) [13] demonstrated the optimal design of PV & wind turbine/biogas fueled diesel generator/battery/electrolyzer hybrid system for producing hydrogen and providing off-grid electricity in a rural West Chinese town. A. A. Zaki Diab et al. (2022) [14] designed optimally a stand-alone microgrid of fuel cell / PV /battery hybrid system to use the most contemporary optimization algorithms equilibrium optimizer, black hole optimization, bat optimization and to supply emergency loads to a nuclear power facility in Egypt. R. S. S. Nuvvula et al. (2022) [15] developed quantum behaved particle swarm optimization, supported by battery energy storage systems and waste-to-energy plant, to get the optimal PV/wind energy conversion system while reducing the techno-economic objectives for an Indian smart city. A. Abbassi et al. (2022) [16] introduced a modified Moth-Flame optimization algorithm as a novel size optimization strategy for PV/Wind hybrid off-grid renewable energy systems connected with a hybrid energy storage system with two different dynamics. That is to improve reliability by minimizing cost of electricity, increasing the renewable energies exploitation energies, and minimizing the LPSP. S. Ayan and H. Toylan (2022) [17] designed a PV/battery / wind hybrid renewable energy system with optimal size for a school building's load demand in Turkey using HOMER Pro software and the artificial bee colony algorithm to acquire the maximum energy output at minimum cost in varying LPSP values. S. Arabi-Nowdeh et al. (2021) [18] examined the optimal design of PV-wind-battery hybrid system that operates in both on- and off-grid modes to meet annual load demand taking into account the emissions, energy generation cost, and the cost of load losses. T. E. K. Zidane et al. (2021) [19] presented optimal sizing of PV array and inverter for large-scale grid-connected PV power plants based on the optimum combination between PV array and inverter to reduce the levelized cost of energy. O. C. Akinsipe et al. (2021) [20] adopted a mathematical modelling for designing using an off-grid photovoltaic system to power a Nigerian home. M. Althani and A. Maheri (2021] [21] proposed an ant colony algorithm for optimal sizing standalone PV- battery - wind diesel-hydrogen based on continuous search space approach. M. Jahannoosh et al. (2021) [22] designed optimal and economic PV/wind turbine/fuel cell hybrid renewable energy system to minimize hybrid system's lifespan cost for supplying residential-commercial centers' demand in Iran. E. T. Marcel et al. (2021) [23] employed an iterative technique to size proposed PV/wind/battery hybrid renewable energy system at minimum annualized cost for a Tanzanian village as a solution for lack of electricity access in developing countries. K. H. Ibrahim et al. (2021) [24] proposed the optimal design of the isolated diesel generator - battery - PV - wind turbine utilizing a genetic algorithm employing design parameters that are PV tilt angle and wind turbine hub height. A. F. Altun and M. Kilic (2020) [25] presented optimal design of renewable-based standalone power system, which includes batteries, wind turbines, an inverter, PV and diesel generator for five areas in Turkey with different climates to supply 5 kW peak electricity demand. B. Berbaoui et al. (2020) [26] proposed a strategy based on viral colony search algorithm for optimal size of stand-alone PV, battery, and diesel generator to decrease equalized cost and reduce the equalized carbon dioxide equivalent life cycle emissions in a remote location of South Algeria. M. Gharibi and A. Askarzadeh (2019) [27] applied a bi-objective optimization approach for sizing a grid-connected PV/ fuel cell / diesel generator hybrid energy system to minimize both levelized cost of energy and LPSP. A. Naderipour et al. (2019) [28] designed optimal hybrid PV, wind, and battery renewable energy system to reduce total net present cost considering loss of load probability as reliability constraint for a city in Iran considering the components outage rate. A. Khan et al. (2019) [29] proposed two enhanced evolutionary sizing algorithms, along with enhanced differential evolution algorithm, teaching-learning based optimization algorithm, and the salp swarm algorithm for sizing PV-WT-battery hybrid renewable energy system in a stand-alone environment to minimize the total annual cost considering the allowable LPSP as a reliability constraint. Z. Movahediyan and A. Askarzadeh (2018) [30] presented a new multiobjective optimization framework to design cost-effective, clean, and reliable PV/diesel generator power system for an isolated area in the operating reserve existence to reduce carbon dioxide emission, total net present cost, and LPSP. N. Ghorbani et al. (2018) [31] applied hybrid genetic technique with particle swarm optimization for the optimal size of an off-grid battery / wind turbine to reduce the total present cost with satisfying load demand considering the LPSP as a reliability factor. A. Maleki et al. (2014) [32] studied optimal sizing of off-grid hybrid diesel /wind/ battery / PV for a remote area electrifying in Iran. The designed system is compared to a dieselpowered generation system in terms of both overall annual cost and environmental emissions.

The literature review makes clear primary focus of the researchers is on hybrid renewable energy systems and their optimal sizing. Motivated by the literature review considerations, the main objectives and contributions of this work are:

- Optimal PV/WT/Batt HRES for residential housing and industrial units in the Egyptian city of Siwa has been designed.
- A new metaheuristic method called RIME technique has been applied to address the optimization issue. The optimization problem utilizes several PV arrays and WTs as decision variables. While the fitness function is minimization of the LPSP.
- The cost analysis has been performed for the optimal system size.
- The statistical analysis for 25 independent runs has been carried out to discuss the effectiveness of the RIME method based on its robustness and convergence curves.

2. System Components

Figure 1 indicates modeling of content of PV/WT/BAT. AC bus and DC bus get the best work to the model, so our work consists of them to get power direct from WTs to the AC load. Energy created with double sources, WTs, and PV is utilized to satisfy client's energy interest. Because of irregular idea of HRESs, a battery bank is likewise coordinated into model. Because of excess energy created by HRESs, batteries are energized to their greatest charging limits. It is important to screen constantly and to survey battery bank charge. The parameters of HRES calculated from Table 1.

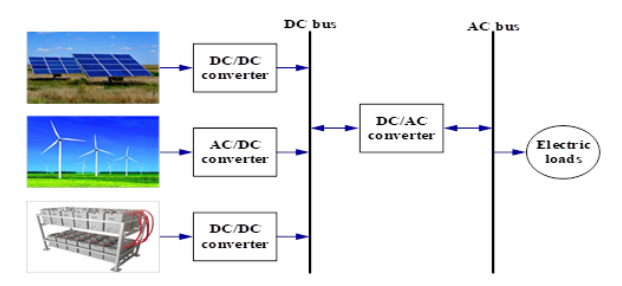


Fig. 1: Proposed hybrid system.

Table 1: Specifications of HRES (Batt / PV / WT) [33-35].

Hybrid system components	Parameters	Value	
PV array	Panel model	BBS24MF400 (Mono PERC)	
	Maximum power	400 W	
	Open circuit voltage	50.49 V	
	Short circuit current	9.98 A	
	No. of panels	13	
	Total capacity	5 kW	
WT	Model	REYAH - H50	
	Rated power	50 kW	
	Frequency	50 Hz	
	Start-up wind speed	3 m/s	
	Rated wind speed	10 m/s	
	Survival wind speed	1 50 m/s	
	Wheel diameter	17.6 m	
Battery	Model	Deep cycle battery	
	Voltage	48 V	
	Nominal capacity	1000 Ah	
	Life span	5	
	Efficiency	95 %	

2.1. Modeling of PV System

PV panel power output (P_{PV}) may be calculated in the following way [36-37],

The total generated energy (kWh) form PV system ($P_{PV-total}$) is determined as follows [38],

$$P_{PV} = \frac{S_G}{S_S} \times P_{PV-array} \times f_{PV}$$
 (1)

$$P_{PV-total} = N_{PV} \times P_{PV} \tag{2}$$

S_G is global incident solar radiation on the panel (kWh/m²),

 S_S is standard incident solar radiation (1 kWh/m²),

 $P_{PV-array}$ is PV array rated capacity (kW),

 f_{PV} is PV derating factor,

 N_{PV} is number of PV arrays.

2.2. Modeling of WT system

The WT generated power (P_{WT}) is obtained as follows [39],

$$P_{WT} = \begin{cases} P_r * \frac{v^3 - v_{low-cut}^3}{v_r^3 - v_{low-cut}^3} & v_{low-cut} \le v \le v_r \\ p_r * nw & v_r \le v \le v_{up-cut} \\ 0 & otherwise \end{cases}$$
(3)

 P_r is wind turbine's nominal power,

v is speed of the wind,

 $v_{low-cut}$ is low speed,

 v_{up-cut} is high speed,

 v_r is acceleration in relation to nominal power.

Variation in wind speed can be obtained from the turbine hub height as follows [11], [40],

$$\frac{\mathbf{v_h}}{\mathbf{v_{h_r}}} = (\frac{\mathbf{h}}{\mathbf{h_r}})^{\epsilon} \tag{4}$$

 v_h (m/s) is the wind speed on average at hub height h (m).

 v_{h_r} (m/s): at the reference height h_r (m), the average wind speed.

 ϵ is roughness factor that has the values from 0.14 to 0.25.

The total generated power (kW) form WTs ($P_{WT-total}$) is determined as follows,

$$P_{WT-total} = N_{WT} \times P_{WT} \tag{5}$$

 N_{WT} is number of WTs.

2.3. Sizing of Storage Batteries

Due to solar energy's uncertain nature of solar energy, design of the battery system is essential for energy storage and sustainability in power production. The battery storage capacity can be calculated from the required load energy (E_L), number of cloudy days (N_c), battery efficiency (η_B), inverter efficiency (η_{inv}), and depth of discharge (DoD) as follows [20],

battery storage capacity =
$$\frac{E_L \times N_c}{DOD \times \eta_{inv} \times \eta_B} (Wh)$$
 (6)

The total number of required batteries (N_{Batt}) can be calculated as follows,

$$N_{Batt} = \frac{battery\ storage\ capacity}{\text{Nominal capacity of one battery}} \tag{7}$$

3. Methodology

3.10bjective Function

Minimization of LPSP is the objective function with decision variables (N_{PV} and N_{WT}) as constrains as follows,

$$N_{PV}^{min} \le N_{PV} \le N_{PV}^{max} \tag{8}$$

$$N_{WT}^{min} \le N_{WT} \le N_{WT}^{max} \tag{9}$$

Where; N_{PV} is number of PV arrays, N_{PV}^{min} is minimum number of PV arrays, N_{PV}^{max} is maximum number of PV arrays, N_{WT}^{max} is number of WTs, and N_{WT}^{max} is maximum number of WTs.

3.2 Objective Function

LPSP is an important metric tool for evaluating the reliability of energy systems. It is generally indicated by the energy ratio deficit to total energy requirement over an extended period. LPSP can be calculated as follows [11-12],

$$LPSP = \frac{P_{load} - P_{generated}}{P_{load}} = \frac{P_{PV} + P_{WT}}{P_{load}}$$
(10)

Where; P_{load} is the load power, $P_{generated}$ is total generated power, P_{PV} is power generated from PV, and P_{WT} is power generated from WT.

3.3 Cost of HRES [24], [38]

$$C_{PV} = CRF \times (N_{PV} \times C_{PVC}) + OMF \times (C_{PVm} \times N_{PV}) \quad (11)$$

$$C_{WT} = CRF \times (N_{WT} \times C_{WTc}) + OMF \times (C_{WTm} \times N_{WT}) \quad (12)$$

Where; C_{PV} is the total PV system cost, C_{WT} is the total WT cost, C_{PVC} is the capital cost of PV system, C_{WTC} is the capital cost of WT, C_{PVm} is the maintenance cost of PV system, C_{WTm} is the maintenance cost of WT.

The capital recovery factor (CRF) as well as operating and maintenance factor (OMF) can be calculated as follows [24],

$$CRF = \frac{i(1+i)^n}{i(1+i)^n - 1} \tag{13}$$

$$OMF = (1+f)^n \tag{14}$$

Where the interest rate is denoted by i, and the lifespan by n. of project.

The cost of battery (C_{Batt}) can calculated as follows [24],

$$C_{Batt} = 1.03 \times CRF(A \times P_B + B \times E_{Batt}) \times N_{Batt} + SFF \times C_{Battr} \times N_{Batt}$$
 (15)

Where; the parameters A, B are power conversion cap. Cost (\$/W) and battery storage systems (\$/Wh), respectively. Parameter A is assumed to be 0.2, and parameter B is assumed to be 0.451 [24]. P_B is power

conversion (W), E_{Batt} is the battery energy (Wh), N_{Batt} is battery number, C_{Battr} is battery replacement cost, and SFF is the replacement factor, which can be computed as below [24],

$$SFF = \frac{i}{(1+i)^{nb} - 1} \tag{16}$$

Where nb is the battery life-time.

3.4 RIME optimization algorithm

The RIME algorithm is an effective metaheuristic algorithm that is inspired by the rime-ice physical phenomenon. Rime-ice is formed when water vapor in the air accumulates but does not condense. At cold temperatures, it freezes and attaches to any object. Simultaneously, owing to the impact of environmental conditions and the pattern of growth, rime-ice is unable to expand endlessly and will cease growing once it reaches a somewhat steady state. Wind speed impacts the rime development pattern to be soft-rime or hard-rime as shown in Figure 2, where ΔABC symbolize the rime growth plane and D1, D2, D3, D4 indicate the rime birth points. Typically, the soft rime is formed by a breeze with low wind speed and varied wind direction as seen by plane Figure 2(a)in the same height. As a result, the soft rime expands erratically and slowly. Hard rime, on the other hand, is created by gales with high wind speed and the same wind direction in the same height plane as shown in Figure 2(b). So, the hard rime grows rapidly in almost the same direction.

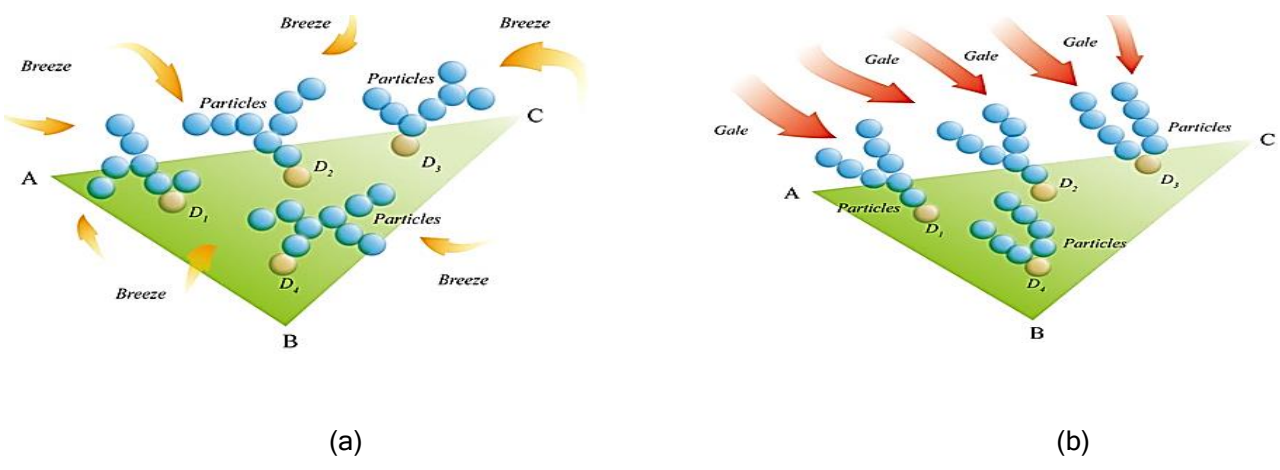


Fig.2: The rime-ice formation process under different environments: (a) soft rime, (b) hard rime [41].

To incorporate exploration and exploitation processes into the optimization techniques, the RIME algorithm utilizes a soft-rime search strategy and a hard-rime puncture mechanism by modeling the soft-rime and hard-rime growth process of rime-ice [41]. The RIME algorithm involves three basic processes [41]:

- Performing the soft-rime particles motion simulation in rime-ice and developing a soft-rime search technique for algorithm exploration.
- Simulate the behavior of crossover amongst hard-rime agents and develop a hard-rime puncture mechanism that is primarily utilized for algorithm exploitation.
- Enhance the algorithm's greedy selection mechanism and develop a positive greedy selection mechanism to introduce suboptimal solutions by altering the optimal solutions selection, thereby the population's inferior solutions are filtered out.

3.4.1 RIME optimization algorithm

RIME algorithm is modeled mathematically by simulating each rime strip's growth involving the impacts of four factors that are wind speed, freezing coefficient, attached material cross-sectional area, and growth time. The motion of rime particles condensing into a rime agent is simulated by modeling each rime particle's motion behavior, resulting in a strip crystal. In the context of that, the RIME algorithm consists of the following four stages,

A. Rime cluster initialization

The whole rime-population is initialized as depicted in Figure 3 and (17) [41]. Each rime-agent's growth state $(F(S_i))$ is considered as the agent's fitness value in the metaheuristic algorithm.

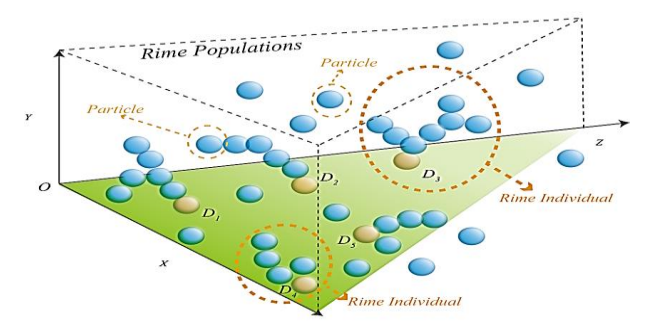


Fig. 3: Initialization of the rime space [41].

$$R = \begin{bmatrix} S_1 \\ S_2 \\ \vdots \\ S_i \end{bmatrix}; S_i = [x_{i1}x_{i2} \cdots x_{ij}] = \begin{bmatrix} x_{11} & x_{12} & \dots & x_{1j} \\ x_{21} & x_{22} & \dots & x_{2j} \\ \vdots & \vdots & \ddots & \vdots \\ x_{i1} & x_{i2} & \dots & x_{ij} \end{bmatrix}$$
(17)

R is the rime-population comprising of n rime agents,

 S_i a rime agent,

i rime number agent,

 x_{ij} rime particle,

j rime number of particle.

B. Soft-rime search strategy

Each rime particle condensation process is mimicked as depicted in Figure 4. The rime particles' location can be formulated as follows [41],

$$R_{ij}^{new} = R_{best.j} + r_1 \cdot \cos \theta \cdot \beta \cdot \left(h \cdot \left(Ub_{ij} - Lb_{ij}\right) + Lb_{ij}\right), r_2 < \sqrt{\left(\frac{t}{T}\right)}$$

$$\theta = \pi \cdot \frac{t}{10 \cdot T}$$

$$\beta = 1 - \frac{\left[\frac{w \cdot t}{T}\right]}{w}$$

$$(20)$$

 R_{ii}^{new} is the updated position of the particle,

i and j indicate the j-th particle of the i-th agent,

 $R_{best,j}$ is the j-th a small portion of the population's greatest agent R,

 r_1 is a random number of ranges from -1 to 1 that controls the particle movement orientation,

h is the coalescence degree that is a random number of ranges from 0 to 1 and controls regulates the distance between the two particles' centers,

 Ub_{ij} and Lb_{ij} are the max and min values of effective particle motion region, respectively,

 r_2 is arbitrary value within the range ([51]),

t is iterations number,

T is the highest quantity of algorithm iterations,

 $[\cdot]$ denotes rounding,

w is a parameter that governs the number of steps segments and has a default value of 5.

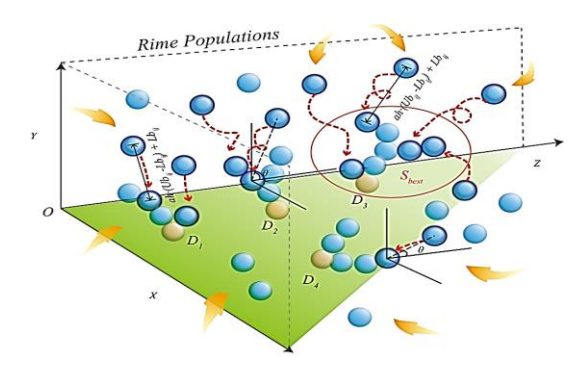


Fig.4: Soft-rime particles motion [41].

C. Hard-rime puncture mechanism

Rime particles condense in the same direction during hard rime formation, allowing rime agents to easily cross over, a process known as rime puncture that is depicted in Figure 5. In well growing conditions, there is a higher likelihood of puncturing between agents. The process of updating the algorithm between agents is inspired by the mechanism of hard-rime puncture. Therefore, the replacement of technique particles and algorithm convergence can be enhanced. The particles replacement can be formulated as follows [41],

$$R_{ij}^{new} = R_{best.j}, r_3 < F^{normr}(S_i)$$
 (21)

 R_{ij}^{new} , $R_{best.j}$ already be defined above,

 r_3 is a random number of ranges from -1 to 1,

 $F^{normr}(S_i)$ is the current agent fitness value's normalized value, representing the likelihood of selecting the *i*-th rime agent.

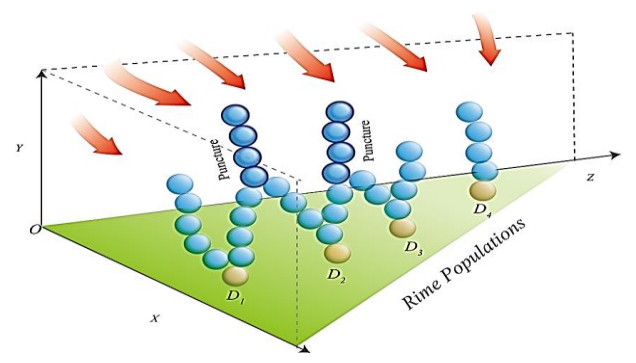


Figure 5. Hard-rime puncturing [41].

D. Positive greedy selection mechanism

To improve exploration efficiency, a greedy selection mechanism has been applied to participate in population updates. The selection process compares the updated agent fitness value to the agent fitness value prior to the update, and in case the modified fitness value is superior, a replacement takes place, and both agents' solutions are changed. Thus, the population's diversity is enhanced, and the algorithm is kept from falling into the local optimum by modifying the optimal solutions selection [41].

E. Applied RIME algorithm

The overall flow chart of the applied algorithm is presented Figure 6.

Fig.6: Flowchart of RIME.

4. Results

In this study, a certain services location in Oasis Siwa (29.150 N, 25.539 E) is considered, which is in Egypt. The site location is connected to a low-reliability electricity grid, limiting the capacity and continuity of electricity supply. The available services of the location conclude schools, farms, and factories. Table 2 shows the load data. Figure 7 depicts the average load profile through the year utilized in the selected case study zone. The maximum load is approximately 100 MW, with a total load of 103 MW.

Table 2: Load data.

Schools' Load data					
Device	Power (W)	All of Power Load (MW)	Quantity		
Appliances (class A "200 W")	500	2	4000		
Appliances (class B "75 W")	1000	5	5000		
Appliances (class C"100 W")	2000	4	2000		
Appliances (class D"50 W")	700	0.7	1000		
Appliances (class E"70 W")	750	3	4000		
Lighting	100	4.3	43000		
	Farms' Load	d data			
Device		Power (MW)			
Total power of operating devices		24			
	Load data of f	actories			
Device		Power (MW)			
Total power of operating devices		60			

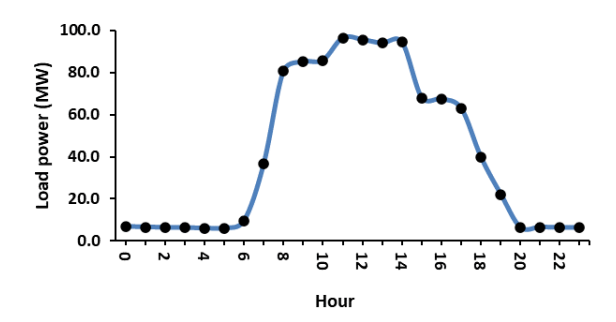


Fig.7: Average Hourly load profile through the year.

The local resources of site location, which include the NASA Surface Meteorology and sun Energy website provided the temperature, wind speed, and sun radiation readings. [42]. Figure 8 depicts solar radiation with average monthly throughout year. June has the highest daily average solar radiation of 8.43 kWh/m²/day. Yearly average solar radiation is 5.92 kWh/m²/day, having an average clarity index of 0.66 that can be utilized all year. Figure 9 represents the average monthly temperature of during year. The yearly average temperature is 21.1 °C, which can affect PV efficiency. Therefore, July's high ambient temperature of 29.68 °C can negatively impact PV panel power generation. Figure 10 shows the monthly average wind speed throughout the year at 50 meters above the ground of earth. The average wind speed throughout a year is 5.53 m/s, indicating that this area has great potential for wind energy utilization.

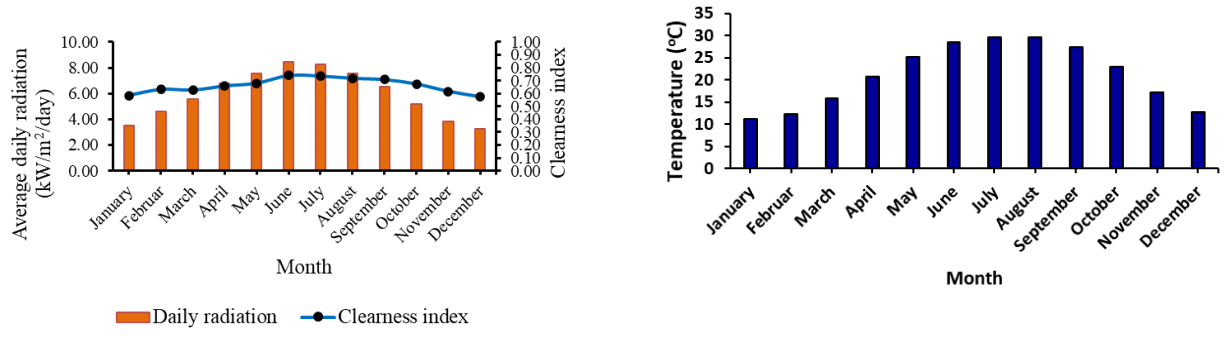


Fig. 8: Average monthly solar radiation.

Fig. 9: Average monthly temperature.

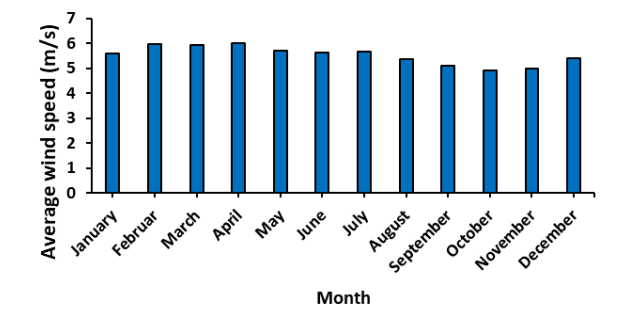


Fig. 10: Average monthly wind speed.

4.1 Discussion

The proposed sizing method is modeled and applied through MATLAB software with considerable variation in the average wind speed, average temperature, and average sun radiation. As input, the model uses solar radiation, temperature, and wind speed measured data from Oasis Siwa location. The decision variables' lowest and maximum limits (number of PV arrays and WTs) are set to 10 and 200, respectively.

Likewise, the used of max and min search agents are 30 and 1000 iterations foe determining the optimal solution for each component, such as solar PV size and WT, Table 3 demonstrates the findings of a simulation of the recommended approach for three techniques. RIME obtained the best optimal solution that forecasts the best COE

of 0.1055 \$/kWh, with lowest NPC = 1.0682×10^7 \$ and LPSP= 1.5×10^{-25} compared to PSO algorithm predictions of 0.9439 \$/kWh to COE, NPC = 3.41×10^7 and LPSP= 6.2973×10^{-9} and CSA which give results for COE= 0.9932, NPC= 5.721×10^8 and LPSP = 9.58373×10^{-7} .

Table 3. The findi	ngs of optimal	l performance value	s outlined b	v RIME and PSO.

Comp.	best Solution	Į.	
	RIME	PSO	CSA
NO PV	98	111	200
COE(\$/kWh)	187	240	88
No WT	0.1055	0.9439	0.9932
NPC	1.0682×10^{7}	3.41×10^7	5.721×10^{8}
LSPS	1.5×10^{-25}	6.2973×10^{-3}	$^{-9}9.58373 \times 10^{-7}$

The comparison demonstrates that the RIME algorithm gives the best COE for 98 PV array and 187 wind turbines. Figure 11 indicates the maximum PV generated power system of about 143 MW and the maximum power generated from wind of about 4 MW. Figure 12 illustrates curve to load demand and the total produced power from both PVs and WTs of the optimized hybrid system.

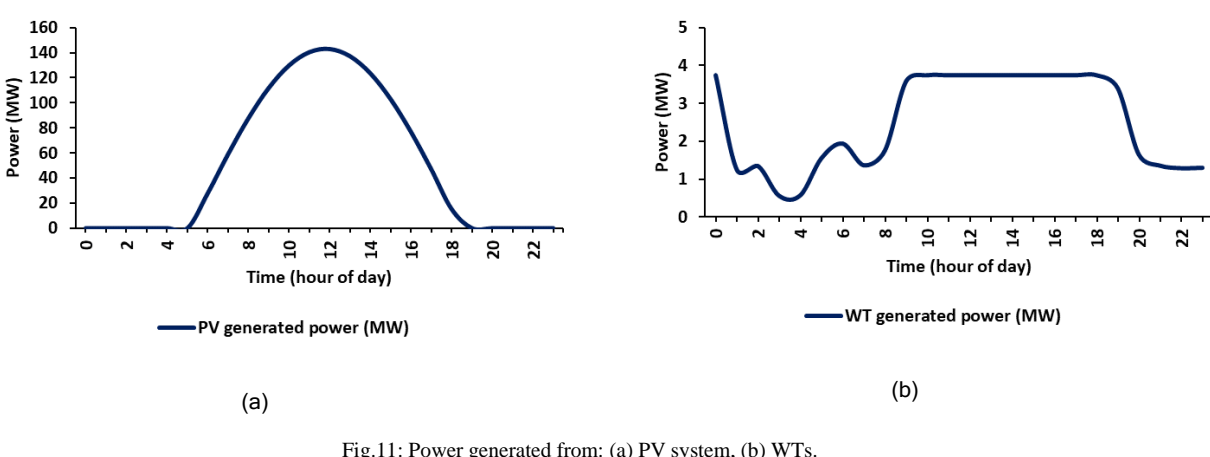


Fig.11: Power generated from: (a) PV system, (b) WTs.

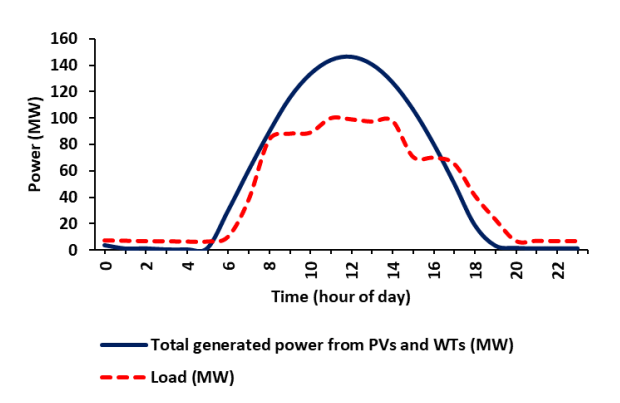


Fig.12: Power generated from PV, WT and Load demand.

The batteries are utilized to increase system reliability and make up for any power deficit in the system by acting as a store device for a continuous supply load. When the total power generated by PVs and WTs exceeds the load demand, the excess electricity is injected into the batteries, which are then in charging mode. When the electricity generated by WTs and PVs is insufficient to meet the load demand, battery discharge is used to compensate. The charge and discharge battery modes depicted in Figure 13.

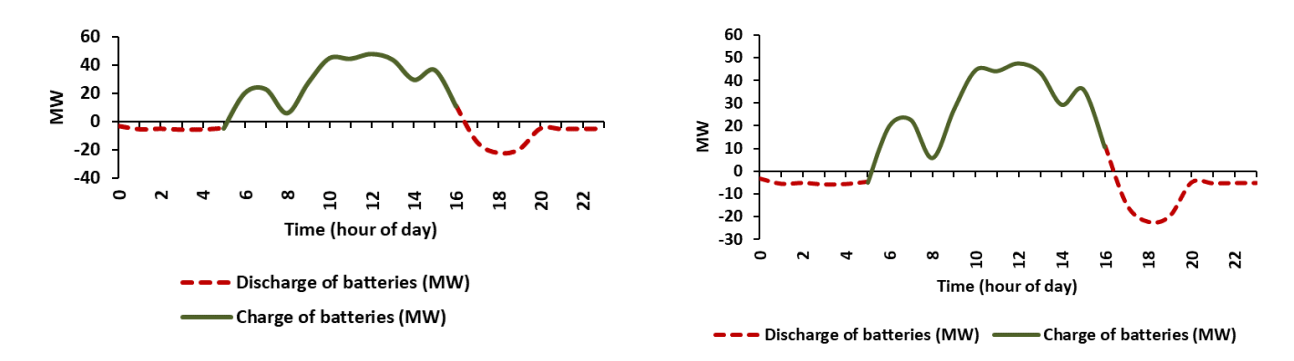


Fig. 13: Charging and discharging of batteries.

Figure 14 shows the process of convergence of RIME algorithm while looking for the best answers to the PV/WT/Batt HRES over 100 independent runs. The convergence occurs at random and stabilizes once the optimal solution is identified. by the 39th iteration. The optimized HRES comprises 98 PV arrays, 187 WTs, and 414 batteries.

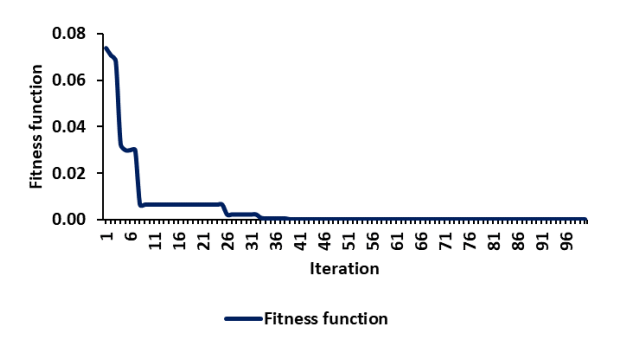


Fig.14: Convergence characteristics of RIME algorithm.

5. Conclusions

This study applies a novel metaheuristic method, called RIME algorithm, for calculating the best size of WT/Batt /PV HRES that is linked to a standalone micro-grid. The objective function is to achieve load demand with lowest LPSP utilizing the number of PV arrays and WTs as decision variables. The optimal sizes of PV arrays, WTs with batteries regarding lowest LPSP are 98, 187, and 414, respectively. The comparison of that new algorithm and two other techniques of PSO and CSA shows the RIME technique gives lowest COE, NPC and LSPS. Future study could focus on diversifying other renewable energy sources in accordance with the site's resources capabilities. Recently found artificial intelligence algorithms can also be utilized.

References

- [1] Liu, X., & Jin, Z. (2020). An analysis of the interactions between electricity, fossil fuel and carbon market prices in Guangdong, China. Energy for Sustainable Development, 55, 82–94. https://doi.org/10.1016/j.esd.2020.01.008.
- [2] Qarnain, S. S., Muthuvel, S., & Bathrinath, S. (2021). Review on government action plans to reduce energy consumption in buildings amid COVID-19 pandemic outbreak. Materials Today: Proceedings, 45, 1264–1268. https://doi.org/10.1016/j.matpr.2020.04.723
- [3] Pradhan, A., Marence, M., & Franca, M. J. (2021). The adoption of Seawater Pump Storage Hydropower Systems increases the share of renewable energy production in Small Island Developing States. Renewable Energy, 177, 448–460. https://doi.org/10.1016/j.renene.2021.05.151
- [4] Movahediyan, Z., & Askarzadeh, A. (2018). Multi-objective optimization framework of a photovoltaic-diesel generator hybrid energy system considering operating reserve. Sustainable Cities and Society, 41, 1–12. https://doi.org/10.1016/j.scs.2018.05.002
- [5] Maleki, A., & Askarzadeh, A. (2014). Optimal sizing of a PV/wind/diesel system with battery storage for electrification to an off-grid remote region: A case study of Rafsanjan, Iran. Sustainable Energy Technologies and Assessments, 7, 147–153. https://doi.org/10.1016/j.seta.2014.04.005
- [6] Alsharif, M. H., Kannadasan, R., Hassan, A. Y., Tawfik, W. Z., Kim, M. K., Khan, M. A., & Solyman, A. A. A. (2022). Optimization analysis of sustainable solar power system for mobile communication systems. Computers, Materials and Continua, 71(2), 3243–3255. https://doi.org/10.32604/cmc.2022.022348

- [7] Sayed, E. T., Wilberforce, T., Elsaid, K., Rabaia, M. K. H., Abdelkareem, M. A., Chae, K. J., & Olabi, A. G. (2021). A critical review on environmental impacts of renewable energy systems and mitigation strategies: Wind, hydro, biomass and geothermal. Science of the Total Environment, 766. https://doi.org/10.1016/j.scitotenv.2020.144505
- [8] Shaban, H., Houssein, E. H., Pérez-Cisneros, M., Oliva, D., Hassan, A. Y., Ismaeel, A. A. K., Abdelminaam, D. S., Deb, S., & Said, M. (2021). Identification of parameters in photovoltaic models through a runge kutta optimizer. Mathematics, 9(18). https://doi.org/10.3390/math9182313
- [9] Abbassi, A., Mehrez, R. ben, Abbassi, R., Saidi, S., Albdran, S., & Jemli, M. (2022). Improved off-grid wind/photovoltaic/hybrid energy storage system based on new framework of Moth-Flame optimization algorithm. International Journal of Energy Research, 46(5), 6711–6729. https://doi.org/10.1002/er.7611
- [10] Li, J., Liu, P., & Li, Z. (2022). Optimal design and techno-economic analysis of a hybrid renewable energy system for off-grid power supply and hydrogen production: A case study of West China. Chemical Engineering Research and Design, 177, 604–614. https://doi.org/10.1016/j.cherd.2021.11.014
- [11] Zidane, T. E. K., Zali, S. M., Adzman, M. R., Tajuddin, M. F. N., & Durusu, A. (2021). PV array and inverter optimum sizing for grid-connected photovoltaic power plants using optimization design. Journal of Physics: Conference Series, 1878(1). https://doi.org/10.1088/1742-6596/1878/1/012015
- [12] Althani, M., & Maheri, A. (n.d.). An Ant Colony Algorithm for HRES Size and Configuration Optimisation.
- [13] Akinsipe, O. C., Moya, D., & Kaparaju, P. (2021). Design and economic analysis of off-grid solar PV system in Jos-Nigeria. Journal of Cleaner Production, 287. https://doi.org/10.1016/j.jclepro.2020.125055
- [14] El-Hady B Kashyout, A., Hassan, A., Hassan, G., El-Banna Fath, H., El-Wahab Kassem, A., Elshimy, H., Ranjanvepa, & Shaheed, M. H. (2021). Hybrid renewable energy/hybrid desalination potentials for remote areas: Selected cases studied in Egypt. In RSC Advances (Vol. 11, Issue 22, pp. 13201–13219). Royal Society of Chemistry. https://doi.org/10.1039/d1ra00989c
- [15] Berbaoui, B., Dehini, R., & Hatti, M. (2020). An applied methodology for optimal sizing and placement of hybrid power source in remote area of South Algeria. Renewable Energy, 146, 2785–2796. https://doi.org/10.1016/j.renene.2019.04.011
- [16] Marcel, E. T., Mutale, J., & Mushi, A. T. (2021). Optimal Design of Hybrid Renewable Energy for Tanzania Rural Communities. Tanzania Journal of Science, 47(5), 1716–1727. https://doi.org/10.4314/tjs.v47i5.19
- [17] Ghorbani, N., Kasaeian, A., Toopshekan, A., Bahrami, L., & Maghami, A. (2018). Optimizing a hybrid wind-PV-battery system using GA-PSO and MOPSO for reducing cost and increasing reliability. Energy, 154, 581–591. https://doi.org/10.1016/j.energy.2017.12.057
- [18] Ibrahim, K. H., Mohamed Ahmed, E., & Saleh, S. M. (2021). Minimum cost-based design of isolated PV-wind hybrid system considering the PV tilt angle and wind turbine hub height as design parameters using genetic algorithm. International Journal of Energy Research, 45(9), 13149–13162. https://doi.org/10.1002/er.6640
- [19] Khan, A., Alghamdi, T., Khan, Z., Fatima, A., Abid, S., Khalid, A., & Javaid, N. (2019). Enhanced Evolutionary Sizing Algorithms for Optimal Sizing of a Stand-Alone PV-WT-Battery Hybrid System. Applied Sciences, 9(23), 5197. https://doi.org/10.3390/app9235197
- [20] Gad, M. S., Said, M., & Hassan, A. Y. (2021). Effect of different nanofluids on performance analysis of flat plate solar collector. Journal of Dispersion Science and Technology, 42(12), 1867–1878. https://doi.org/10.1080/01932691.2020.1845959
- [21] Li, J., Zhao, J., Chen, Y., Mao, L., Qu, K., & Li, F. (2023). Optimal sizing for a wind-photovoltaic-hydrogen hybrid system considering levelized cost of storage and source-load interaction. International Journal of Hydrogen Energy, 48(11), 4129–4142. https://doi.org/10.1016/j.ijhydene.2022.10.271
- [22] Hassan, A. Y., Ismaeel, A. A. K., Said, M., Ghoniem, R. M., Deb, S., & Elsayed, A. G. (2022). Evaluation of Weighted Mean of Vectors Algorithm for Identification of Solar Cell Parameters. Processes, 10(6). https://doi.org/10.3390/pr10061072
- [23] Mahmoud, F. S., Diab, A. A. Z., Ali, Z. M., El-Sayed, A. H. M., Alquthami, T., Ahmed, M., & Ramadan, H. A. (2022). Optimal sizing of smart hybrid renewable energy system using different optimization algorithms. Energy Reports, 8, 4935–4956. https://doi.org/10.1016/j.egyr.2022.03.197
- [24] Ayan, S., & Toylan, H. (2022). Size optimization of a stand-alone hybrid photovoltaic/wind/battery renewable energy system using a heuristic optimization algorithm. International Journal of Energy Research, 46(11), 14908–14925. https://doi.org/10.1002/er.8192
- [25] Zaki Diab, A. A., El-Rifaie, A. M., Zaky, M. M., & Tolba, M. A. (2022). Optimal Sizing of Stand-Alone Microgrids Based on Recent Metaheuristic Algorithms. Mathematics, 10(1). https://doi.org/10.3390/math10010140
- [26] Jahannoosh, M., Nowdeh, S. A., Naderipour, A., Kamyab, H., Davoudkhani, I. F., & Klemeš, J. J. (2021). New hybrid meta-heuristic algorithm for reliable and cost-effective designing of photovoltaic/wind/fuel cell energy system considering load interruption probability. Journal of Cleaner Production, 278. https://doi.org/10.1016/j.jclepro.2020.123406
- [27] Nuvvula, R. S. S., Devaraj, E., Madurai Elavarasan, R., Iman Taheri, S., Irfan, M., & Teegala, K. S. (2022). Multiobjective mutation-enabled adaptive local attractor quantum behaved particle swarm optimisation based optimal sizing of hybrid renewable energy system for smart cities in India. Sustainable Energy Technologies and Assessments, 49. https://doi.org/10.1016/j.seta.2021.101689
- [28] Arabi-Nowdeh, S., Nasri, S., Saftjani, P. B., Naderipour, A., Abdul-Malek, Z., Kamyab, H., & Jafar-Nowdeh, A. (2021).
 Multi-criteria optimal design of hybrid clean energy system with battery storage considering off- and on-grid application.
 Journal of Cleaner Production, 290. https://doi.org/10.1016/j.jclepro.2021.125808
- [29] Altun, A. F., & Kilic, M. (2020). Design and performance evaluation based on economics and environmental impact of a PV-wind-diesel and battery standalone power system for various climates in Turkey. Renewable Energy, 157, 424– 443. https://doi.org/10.1016/j.renene.2020.05.042

- [30] Gharibi, M., & Askarzadeh, A. (2019). Technical and economical bi-objective design of a grid-connected photovoltaic/diesel generator/fuel cell energy system. Sustainable Cities and Society, 50. https://doi.org/10.1016/j.scs.2019.101575
- [31] Wankouo Ngouleu, C. A., Koholé, Y. W., Fohagui, F. C. V., & Tchuen, G. (2023). Optimal sizing and techno-enviro-economic evaluation of a hybrid photovoltaic/wind/diesel system with battery and fuel cell storage devices under different climatic conditions in Cameroon. Journal of Cleaner Production, 423. https://doi.org/10.1016/j.jclepro.2023.138753
- [32] Naderipour, A., Abdul-Malek, Z., Zahedi Vahid, M., Mirzaei Seifabad, Z., Hajivand, M., & Arabi-Nowdeh, S. (2019). Optimal, Reliable and Cost-Effective Framework of Photovoltaic-Wind-Battery Energy System Design Considering Outage Concept Using Grey Wolf Optimizer Algorithm Case Study for Iran. IEEE Access, 7, 182611–182623. https://doi.org/10.1109/ACCESS.2019.2958964
- [33] https://bluebirdsolar.com/products/bluebird-5kw-solar-panels.
- [34] https://www.taqetna.com/wp-content/uploads/2020/06/REYAH50-Wind-Turbine-Datasheet.pdf.
- [35] https://www.foreverpureplace.com/24-125-11-FLA-p/24-125-11.fla.htm.
- [36] Ma, T., Yang, H., & Lu, L. (2014). A feasibility study of a stand-alone hybrid solar-wind-battery system for a remote island. Applied Energy, 121, 149–158. https://doi.org/10.1016/j.apenergy.2014.01.090
- [37] Maleki, A., & Pourfayaz, F. (2015). Optimal sizing of autonomous hybrid photovoltaic/wind/battery power system with LPSP technology by using evolutionary algorithms. Solar Energy, 115, 471–483. https://doi.org/10.1016/j.solener.2015.03.004
- [38] Moghaddam, S., Bigdeli, M., Moradlou, M., & Siano, P. (2019). Designing of stand-alone hybrid PV/wind/battery system using improved crow search algorithm considering reliability index. International Journal of Energy and Environmental Engineering, 10(4), 429–449. https://doi.org/10.1007/s40095-019-00319-y
- [39] Su, H., Zhao, D., Heidari, A. A., Liu, L., Zhang, X., Mafarja, M., & Chen, H. (2023). RIME: A physics-based optimization. Neurocomputing, 532, 183–214. https://doi.org/10.1016/j.neucom.2023.02.010
- [40] Tazay, A. F., Ibrahim, A. M. A., Noureldeen, O., & Hamdan, I. (2020). Modeling, control, and performance evaluation of grid-tied hybrid pv/wind power generation system: Case study of gabel el-zeit region, egypt. IEEE Access, 8, 96528– 96542. https://doi.org/10.1109/ACCESS.2020.2993919
- [41] Mahmoud, F. S., Abdelhamid, A. M., al Sumaiti, A., El-Sayed, A. H. M., & Diab, A. A. Z. (2022). Sizing and Design of a PV-Wind-Fuel Cell Storage System Integrated into a Grid Considering the Uncertainty of Load Demand Using the Marine Predators Algorithm. Mathematics, 10(19). https://doi.org/10.3390/math10193708
- [42] NASA Surface meteorology and solar energy; Available from: http://eosweb.larc.nasa.gov/sse/.